



OPEN

## VADER: a variable dose-rate external $^{137}\text{Cs}$ irradiator for internal emitter and low dose rate studies

Guy Garty<sup>1,2</sup>✉, Yanping Xu<sup>1,8</sup>, Gary W. Johnson<sup>2</sup>, Lubomir B. Smilenov<sup>2</sup>, Simon K. Joseph<sup>3</sup>, Monica Pujol-Canadell<sup>2</sup>, Helen C. Turner<sup>2</sup>, Shanaz A. Gandhi<sup>2</sup>, Qi Wang<sup>2</sup>, Rompin Shih<sup>4</sup>, Robert C. Morton<sup>2</sup>, David E. Cuniberti<sup>2</sup>, Shad R. Morton<sup>2</sup>, Carlos Bueno-Beti<sup>2</sup>, Thomas L. Morgan<sup>5</sup>, Peter F. Caracappa<sup>5</sup>, Evagelia C. Laiakis<sup>6,7</sup>, Albert J. Fornace Jr.<sup>6,7</sup>, Sally A. Amundson<sup>2</sup> & David J. Brenner<sup>2</sup>

In the long term,  $^{137}\text{Cs}$  is probably the most biologically important agent released in many accidental (or malicious) radiation disasters. It can enter the food chain, and be consumed, or, if present in the environment (e.g. from fallout), can provide external irradiation over prolonged times. In either case, due to the high penetration of the energetic  $\gamma$  rays emitted by  $^{137}\text{Cs}$ , the individual will be exposed to a low dose rate, uniform, whole body, irradiation. The VADER (VARIABLE Dose-rate External  $^{137}\text{Cs}$  irradiator) allows modeling these exposures, bypassing many of the problems inherent in internal emitter studies. Making use of discarded  $^{137}\text{Cs}$  brachytherapy seeds, the VADER can provide varying low dose rate irradiations at dose rates of 0.1 to 1.2 Gy/day. The VADER includes a mouse “hotel”, designed to allow long term simultaneous residency of up to 15 mice. Two source platters containing ~ 250 mCi each of  $^{137}\text{Cs}$  brachytherapy seeds are mounted above and below the “hotel” and can be moved under computer control to provide constant low dose rate or a varying dose rate mimicking  $^{137}\text{Cs}$  biokinetics in mouse or man. We present the VADER design and characterization of its performance over 18 months of use.

In many large-scale radiation exposure scenarios,  $^{137}\text{Cs}$  is often the major source of internal or external radiation exposure<sup>1–3</sup>.  $^{137}\text{Cs}$  is generated in large quantities by fission and is one of the major sources of contamination following reactor accidents<sup>3</sup> and in nuclear fallout, for ground burst nuclear detonations<sup>4</sup> (but not for air burst scenarios<sup>5</sup>). Due to its ubiquity in industrial irradiation systems, it presents a hazard for both malicious and accidental release (similar to the Goiânia accident<sup>6</sup>).

$^{137}\text{Cs}$  is a water-soluble  $\gamma$  emitter with a physical half-life of 30 years. When released, it can readily be deposited on surfaces and enter the food chain<sup>7,8</sup>. Because of its environmental persistence and ease of dispersal,  $^{137}\text{Cs}$  poses a significant risk to the general public. It is therefore important to develop biological assays for identifying individuals exposed to internal or environmental  $^{137}\text{Cs}$ . With external exposures, following an improvised nuclear device (IND) for example, dose rates may be initially high, depending on the level of shielding and distance from the detonation<sup>9</sup>, and decrease rapidly with time<sup>10</sup>, following the so called 7–10 rule<sup>11</sup>, which is a consequence of the various decay times of the wide range of isotopes released. Typical exposure durations are on the order of 48 h to 1 week, depending on the time required for evacuation, and doses of multiple Gy over this period are possible<sup>9</sup>.

In the case of internal exposures, dose rates are typically much lower<sup>4</sup> but the persistence may be much higher:  $^{137}\text{Cs}$  permeates all tissues and is cleared over a period of months<sup>12</sup> (although chelating agents somewhat accelerate its clearance<sup>13</sup>), accumulating damage to tissues and particularly to the genetic material, which may result in delayed disease. Thus, in the event of a large-scale accidental or malicious release of volatile radionuclides, resulting in internal or external exposures, there is an important need to develop radiation biodosimetry assay(s) and technologies for population-based triage and subsequent dose-dependent medical management<sup>2</sup>.

<sup>1</sup>Radiological Research Accelerator Facility, Columbia University, 136 S. Broadway, Box 21, Irvington, NY 10533, USA. <sup>2</sup>Center for Radiological Research, Columbia University, New York, NY 10032, USA. <sup>3</sup>David A. Gardner PET Imaging Research Center, Columbia University, New York, NY 10032, USA. <sup>4</sup>Department of Radiation Oncology, Columbia University, New York, NY 10032, USA. <sup>5</sup>Environmental Health and Safety, Columbia University, New York, NY 10032, USA. <sup>6</sup>Department of Oncology, Lombardi Comprehensive Cancer Center, Georgetown University, Washington DC 20057, USA. <sup>7</sup>Department of Biochemistry and Molecular and Cellular Biology, Georgetown University, Washington DC 20057, USA. <sup>8</sup>Yanping Xu is deceased. ✉email: gyg2101@cumc.columbia.edu

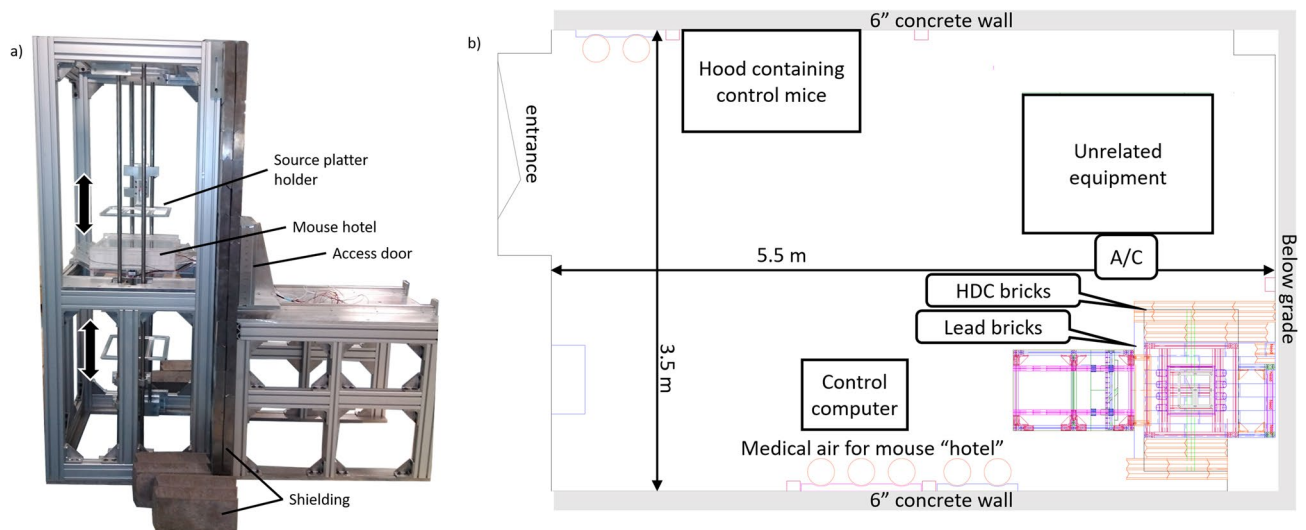


**Figure 1.** (a) Photo of the VADER structure before installation of the shielding. (b) schematic of the VADER room layout.

Over the past decade, we have utilized  $^{137}\text{CsCl}_{(\text{aq})}$  injection in mice to study the long-term effects of ingested  $^{137}\text{Cs}$  on cytogenetic<sup>14,15</sup>, transcriptomic<sup>16</sup> and metabolomic<sup>17,18</sup> endpoints. The difficulty of these studies lies in the fact that both the study animals and the resulting biofluids are often radioactive and require dedicated equipment to analyze, making systematic studies difficult and expensive. At this time, only one or two laboratories in the US have the appropriate facilities and highly trained personnel that are required for conducting these  $^{137}\text{Cs}$  injection studies.

As the majority of dose delivered from this type of exposure is due to long range  $\gamma$  rays<sup>19</sup> (Half Value Layer: 82 mm in water<sup>20</sup>), the physical dose distribution will be very similar for internal vs. external  $^{137}\text{Cs}$  exposures. Thus, it is possible to model internal exposures (e.g. from ingested fallout) using an external isotope source, provided it is properly modulated to model biokinetics<sup>21</sup>.

We have developed the VADER (VARIABLE Dose-rate EXternal  $^{137}\text{Cs}$  irradiatoR) to facilitate modeling of low dose rate  $^{137}\text{Cs}$  exposures either from ingested or fallout exposures. Our aim was to allow arbitrary dose time profile exposures (mimicking biokinetic clearing<sup>12</sup>, the 7:10 rule<sup>11</sup>, constant prolonged dose rate, etc.) to 15 mice at a time, without generating radioactively contaminated biofluids. As such we believe the VADER to be a useful tool for the radiation research community in investigating the effects of prolonged, low dose rate, low LET irradiations.

The VADER irradiator is based on “repurposing” of old  $^{137}\text{Cs}$  brachytherapy seeds. These seeds were much used starting in the 1980s to treat cervical cancer at low dose rate<sup>22</sup>, but are no longer in use clinically and so the seeds are kept in long-term storage, making them available for research use. At Columbia University, we had available a few dozen such sources, ranging from 3 to 35 mCi each. We describe below the construction and first two years of operation of the VADER system, including several 30-day mouse irradiations, designed to mimic the internal exposure experiments described in<sup>15–18</sup>.

## VADER design

**Overview.** The VADER system (shown in Fig. 1a) was designed around the requirement to house 15 mice at a time in an environment with dose rates of up to approximately 1 Gy/day over a period of several weeks. The VADER geometry was therefore dictated by a balance between the size of the mouse “hotel”, which should be as large as possible to accommodate as many mice as possible, and the requirement to provide the required dose rate uniformly over its area, using available sources. Within the hotel, mice are free to move around, eat and drink ad libitum. Temperature, humidity, airflow and lighting are fully controlled to the required animal care standards (20–25 °C; 30–70% humidity). Shielding is provided by a mixture of lead and high-density concrete bricks as described below.

Approximately 0.5 Ci of  $^{137}\text{Cs}$  brachytherapy seeds, divided between two platters (above and below the mouse “hotel”), can be moved from almost touching the mouse “hotel” to about 60 cm above and below it, allowing a time-variable dose rate to be implemented. Arrangement of the sources within the platter was optimized to achieve as uniform as possible a radiation field at about 1 Gy/day.

A feature of the VADER is that there are no fixed active components within the VADER enclosure. All environmental controls and monitoring are integrated into the removable mouse “hotel” so that they can be easily replaced in case of radiation damage. This is significantly cheaper and easier than using radiation hardened sensors and electronics. Similarly, the motors driving the source holders are placed outside the shielding and the platters are moved using steel cables and pulleys.

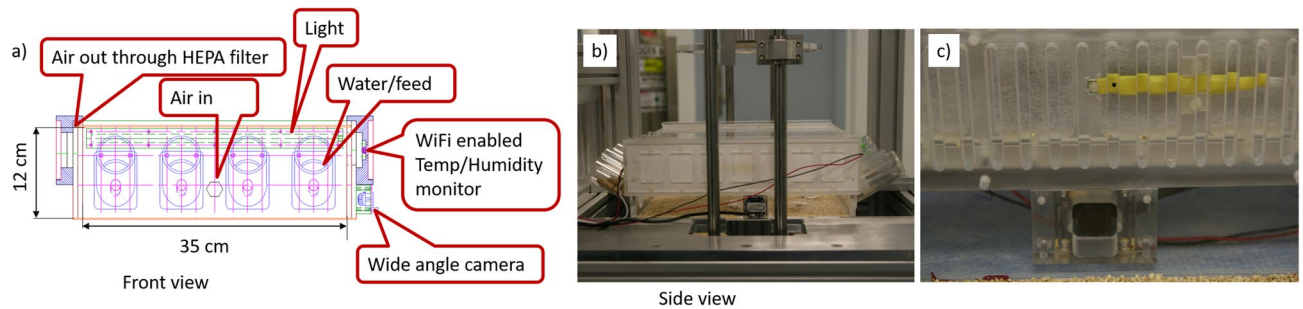


**Figure 2.** (a) design drawing (front view) of the mouse “hotel”. Air inlet and outlet, feeders, illumination, temperature/humidity sensor and camera are indicated. (b) side view photo (taken from the right of panel a). (c) close up of temperature and humidity sensor, photo taken from inside the right side of the “hotel”.

**Design of the mouse “hotel”.** A custom mouse “hotel” (Fig. 2) was designed with the goal of housing up to 15 mice for 5–7 days at a time (with longer residencies requiring periodic cleaning and replenishment of food and water). The “hotel” therefore consists of a 35 cm × 35 cm × 12 cm acrylic box in which the mice are free to move and interact with each other. Mice are able to eat and drink ad libitum from four all-plastic, custom-made water bottles and reservoirs holding feed pellets placed behind glass rods. Sufficient bedding material is also provided within the mouse “hotel”. Real time monitoring of the mice is performed using a 180° fisheye USB camera (ELP, Amazon) embedded into one of the “hotel” walls.

Four mouse “hotels” were built: two to be used simultaneously (one inside the VADER, and one for the zero dose control mice) and two spares to allow the weekly rapid transfer of the mice into a clean “hotel” with fresh bedding and replenished food and water.

To monitor the environment in the mouse “hotel”, a temperature/humidity sensor (HWg HTemp, TruePath Technologies Victor, NY) is integrated into one of the “hotel” walls. Medical grade air is piped into the “hotel” at a rate of 1.5 L/min (10 volume changes/h). Used air is vented into the VADER enclosure through two 100 cm<sup>2</sup> HEPA filters (M-Bar Filter, Allentown Inc, Allentown, NJ). A day-night light cycle is maintained by integrating Warm White (3100 K) LEDs (SMD3528; LEDWholesalers, Hayward, CA) into the “hotel” walls. The LEDs are powered using an adjustable benchtop power supply (Laskar Electronics, Erie, PA), plugged into a Tork timer (Grainger, Lake Forest, IL). The timer was set to “on” between 8 AM and 8 PM and “off” between 8 PM and 8 AM. Light intensity was adjusted to 60 lx.

**Design of the irradiation system.** When designing the source arrangement, our goal was to achieve a maximal dose of 1 Gy/day (we can provide higher dose rates using a highly filtered X-ray machine<sup>23</sup>) with a uniformity of ± 10% or better across the mouse “hotel”. As the VADER system is based on repurposing of existing <sup>137</sup>Cs brachytherapy seeds, we were limited to use available sources, which vary in age, intensity and physical dimensions: The seeds available to us ranged between 3 and 35 mCi, as verified using a well counter (HDR 1000 plus, Standard Imaging Inc, Middleton, WI), and were either 20.0 or 21.0 mm long and between 3.1 and 3.2 mm in diameter.

To model various source geometries and select the seed intensities and positions, we calculated the expected dose across the mouse “hotel” using a MATLAB script. We modeled each seed as two point sources 7 mm apart. The dose rate at a distance  $R$  from each half seed is given by

$$\text{Dose rate [Gy/day]} = 67.92 \frac{\frac{1}{2} \text{Seed activity [mCi]}}{R[\text{mm}]^2} \quad (1)$$

where 67.92 is the dose rate in Gy/day, 1 mm away from a 1 mCi <sup>137</sup>Cs point source, obtained using the RadPro Calculator (<https://www.radprocalculator.com/Gamma.aspx>) and a quality factor of 1.

The ideal source placement above and below the mouse “hotel”, within the geometric and source availability constraints is shown in Fig. 3. Eight sets of three 20 mm long seeds, totaling about 50 mCi per set were placed above/below the four corners of the mouse “hotel” and single 21 mm long 10–17 mCi seeds at the centers of the edges and at the center of the “hotel”. Using this geometry, the dose rate within the mouse “hotel” was calculated to be uniform to within 20% at the highest nominal dose rate (1 Gy/day), as seen in Fig. 3b.

Custom aluminum platters (Protolabs, Maple Plain, MN; Fig. 4) were designed to hold the seeds. Each platter consists of two 27.8 cm wide square aluminum frames (4.75 mm and 3.2 mm thick) with pockets hollowed out for the seeds. Openings were made on both frames so that, while the seeds are captive, between the two frames, there is no material between the active portion of the seed and the mouse “hotel”, regardless of platter orientation.

The seeds were arranged such that three 20 mm long seeds are placed at the corners, and one 21 mm long seed is placed at the center of each edge and at the platter center. Grouping seeds by size in this way simplified the design and allowed tighter tolerances on the pocket lengths, preventing the seeds from shifting or falling out during use.

The seeds were loaded into the platters using remote manipulators at Columbia University’s David A. Gardner PET Imaging Research Center. Once the seeds were loaded into the platter and the platter lid connected, the platters were loaded into a lead safe (MarShield, Burlington, ON) and transported to the VADER location.

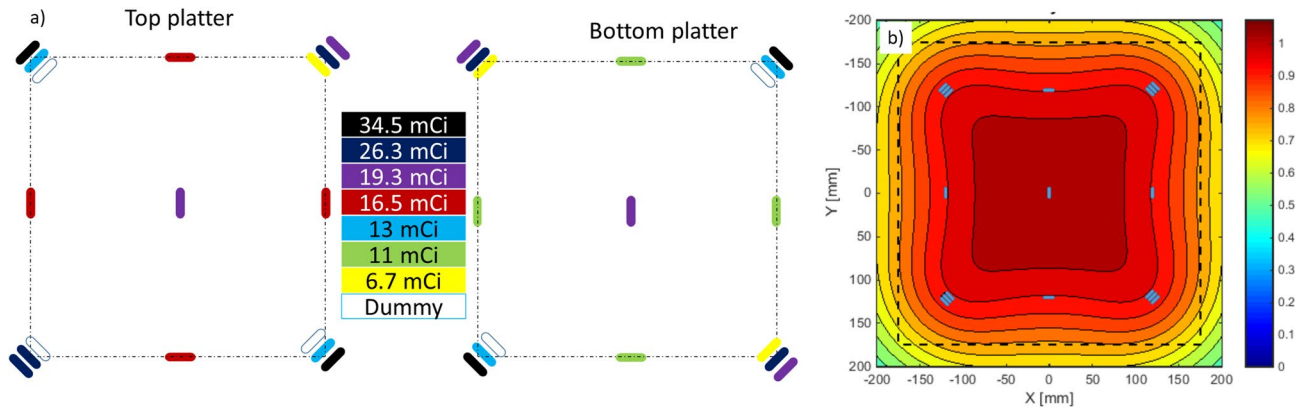


**Figure 3.** (a) The source arrangement used in VADER. (b) MATLAB simulation of the dose rate obtained from this arrangement. The dashed line corresponds to the extents of the mouse “hotel”; each contour corresponds to a 5% variation in expected dose rate.

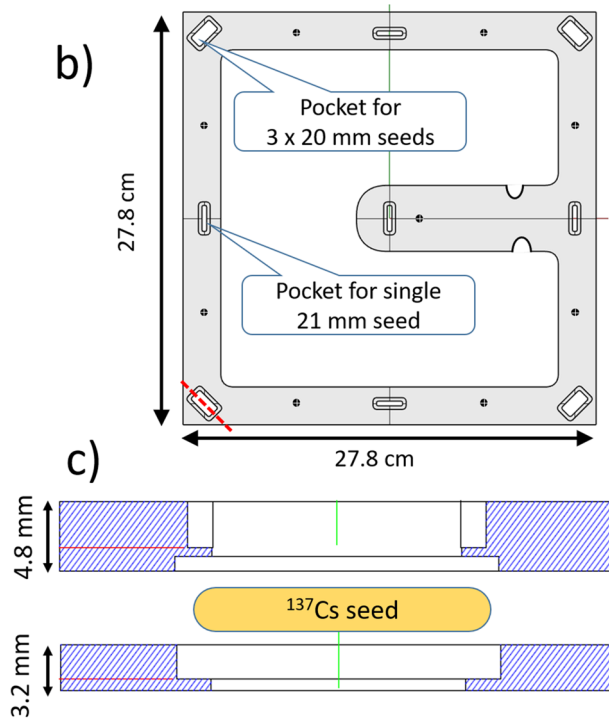
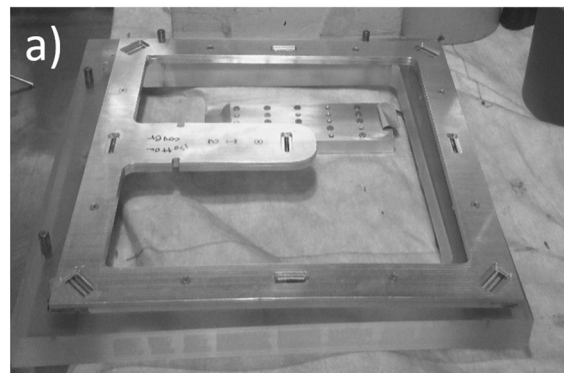


**Figure 4.** (a) photo of the seed holder plate with seeds loaded at the hot cell. (b) Top view design drawing of one of the aluminum frames. (c) Exploded side view cross-section, along the red dotted line in (b), showing both frames and one seed.



Loading the platters into the safe and transferring the platters into the VADER were achieved using a 5' long rod with a gripper, that locks onto notches in the central column of the platter, and supervised by Columbia University's Radiation Safety Office.

Within the VADER, the seed platters sit on a frame that is free to move along a vertical Steel rod, using linear ball bearings. Two Motors (AZM46MC-TS10, Oriental Motors USA Corp., Torrance, CA) are mounted outside the shielding, above the VADER. Each motor controls a spool of 3/32" ultra-flexible stainless-steel wire rope (150 lb capacity, McMaster-Carr, Princeton, NJ) used to raise and lower the source platters.

The stepper motors include an absolute mechanical encoder, allowing repeatable absolute positioning, without battery back-up or external sensors. The motors also include an electromagnetic brake, which activates when power is removed. This allows the source platter to stay in place (rather than falling) in the case of a power failure. A built in 10:1 Taper hobbled gearbox provides a torque of up to 2 Nm and a motion of 0.036°/Pulse (17 cm/turn). Each motor is independently controlled by an AZD-AD Motor driver (Oriental Motors). The two drivers are daisy-chained and controlled by RS485 Modbus.

A second steel cable connects each platter to an external counterweight and allows external verification of the source position, independent of the motor encoder. The motor encoders were configured such that they read zero (home) at the fully retracted position. This allows for a rapid retraction of the sources using the controller's ZHOME (fast return to home) command.

**Shielding design.** Minimizing radiation exposure to the operators and other uninvolved personnel is a prime concern in the design of  $^{137}\text{Cs}$ -based irradiators. Shielding for the VADER was designed to maintain radiation doses to occupationally exposed personnel (operators) in the room below 0.1 mGy/wk and 0.02 mGy/wk to anyone outside the room, in accordance with the guidance of NCRP Report 151<sup>24</sup>. This also allows non-irradiated, control, mice to be housed in the same room (Fig. 1b).

The room where VADER is installed is below grade, such that the rear wall is the building's perimeter foundation wall. Adjacent rooms to the east and west and above are uncontrolled areas and considered occupied by uninvolved personnel (i.e., general public). An uncontrolled corridor borders the south side of the room. The walls are constructed of normal density concrete, 6" thick; the floor above is 4" of normal concrete.

In consultation with Columbia University's Radiation Safety Office, we have determined the required shielding to be either 3" of lead or 12" of high-density concrete (4.7 g/cm<sup>3</sup>; HDC). The side walls of VADER were built of two layers of 6" × 6" × 12" HDC interlocking bricks (Ultradray Inc, Oakville, ON, seen at the bottom of Fig. 1). Half bricks were used to offset the vertical seam every other row, to increase structural stability. An external aluminum frame was provided to increase lateral stability of the walls. The front and top faces of the VADER, however, required penetrations for inserting/removing the mouse "hotel" as well as for control cables and were therefore made of lead, which is much more expensive but can be machined. We used 1.5" × 4" × 12" interlocking lead bricks (Radiation Protection Products Inc. Wayzata, MN), similarly arranged in two layers with half bricks used to offset the seams. A custom sliding door made of a 3" thick lead slab, held in an aluminum frame was designed and built, to allow access to the mouse "hotel". Although heavy, the door slides on rails and can be easily opened and closed with one hand. The rear face of the irradiator was not shielded as it abuts the north wall, is below grade and hence, there are no occupied spaces beyond.

**VADER control and monitoring.** Control software for the VADER was written in Visual C++ (Microsoft, Redmond, WA). The software consists of a single windows "form" that controls the source movement and camera as well as monitoring the temperature and humidity in the mouse "hotel". The PC running the VADER control software was configured to allow for secure remote access to allow monitoring of VADER operations from offsite.

As an experiment could last 30 days or more, it is crucial to allow recovery from unforeseen computer reboots (e.g. system updates or power failures). The VADER control software was therefore configured to automatically start at computer start up (prior to login) and maintain files containing the start time of irradiation and the required irradiation profile: a list of required source positions as a function of time. During operation, the control software periodically compares the elapsed time since the beginning of the experiment to this list and verifies that the positions reported by the motors correspond to the required ones, moving the sources if necessary. The motor position and status as well as the temperature and humidity probe values, are displayed on screen and saved to a comma separated variable (csv) log file, which can be imported into excel.

## Dosimetry

Offline dosimetry of the VADER was performed using an ionization chamber (10 × 6–6, Radcal Corp., Monrovia, CA) calibrated to measure Air-Kerma. Following a background measurement outside the VADER the ionization chamber and electrometer were placed at the center of the mouse "hotel" and dose integrated for 5 min at each retraction position. Annual repeat measurements gave dose rates consistent with the expected 2.3%/year decay of the seeds (Fig. 5). The required retraction as a function of dose rate was interpolated by fitting to a third order polynomial. When monitoring VADER operations, the nominal dose rate was calculated based on the source position and ionization chamber results.

Dose uniformity was evaluated using EBT3 radiochromic film (Ashland Advanced Materials, Bridgewater, USA). Four 17.5 cm square pieces of film were taped down at the bottom of the mouse "hotel" and exposed for several days. Films were scanned on a 48 Bit RGB Epson Perfection V700 Photo flatbed scanner (Epson, Japan), with a resolution of 300 dpi. We used the web application [radiochromic.com](http://radiochromic.com)<sup>25</sup> to analyze the films. The program used a set of calibration films, obtained by exposing film to known doses of 250 kVp X-rays, to define a

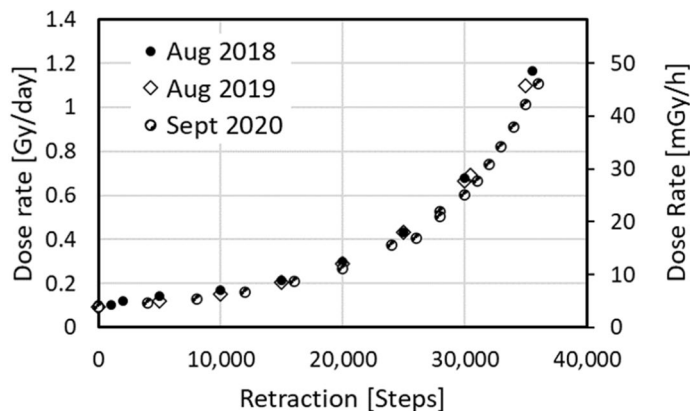


**Figure 5.** Dose rate as a function of reported motor position, measured using an ionization chamber in 1st tests of the VADER (solid symbols), one year later (open symbols) and two years later (half open symbols). We expect a 2.3% decay per year due to the half life of  $^{137}\text{Cs}$ .

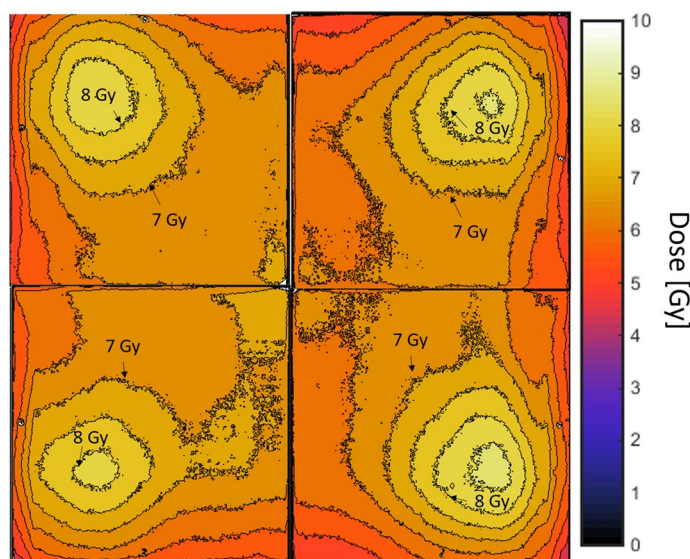


**Figure 6.** Field uniformity, as measured using Gafchromic film at the highest dose rate (1.2 Gy/day). The four panels correspond to four 17.5 cm square films exposed simultaneously, covering the entire mouse “hotel” area. Contours correspond to 0.5 Gy (roughly 5%) steps.

relationship between the optical density of the three colors and a given dose. The two-dimensional dose distribution for a given film could then be determined using this relationship with high accuracy.

Figure 6 shows the dose uniformity across the surface of the mouse “hotel” at the highest dose rate. Variation of measured dose across the film is 10% (standard deviation). Hot spots are evident near the 50 mCi source clusters at the highest dose rates. These average out as the sources retract from the “hotel”; at 1 Gy/day the standard deviation across the “hotel” was reduced to 3.5%.

In vivo dosimetry was performed on a mouse-by-mouse basis, by injecting a glass encapsulated TLD chip into each mouse<sup>26</sup>. After irradiation, the TLD rods were read on a Harshaw 2500 TLD reader (Thermo Fisher Scientific), using the recommended heating profile (5 °C/s ramp to 300 °C, hold at 300 °C and cool to 50 °C). Dose was reconstructed as described in<sup>26</sup>.

### Mouse studies

All animal experiments were approved by the Columbia University Institutional Animal Care and Use Committee (IACUC; approved protocol AAQ2410) and were conducted under all relevant federal and state guidelines.

Before starting any biological study for biodosimetry endpoints, we placed 15 mice into the mouse “hotel” and monitored them over 2 weeks. No weight loss and normal food and water consumption was found. Initially, the mice were exploratory in the new environment and after about 30 min settled down. Similar behavior was observed in the VADER experiments.

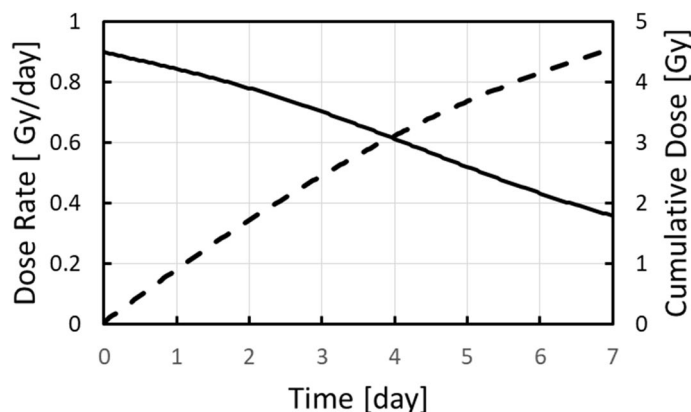


**Figure 7.** VADER programming for a 1 week run. The solid curve (left axis) displays the target dose rate as a function of time. The dashed curve (right axis) displays the target cumulative dose as a function of time.

Day	Dose rate [Gy/day]	Nominal dose [Gy]	Average TLD dose [Gy]
1	0.84	0.87	0.66 ± 0.03
4	0.6	3.1	2.5 ± 0.3
7	0.36	4.5	4.33 ± 0.14

**Table 1.** Dose rates and doses for the one-week study.

**Mouse handling.** For a typical experiment, 30 (15 irradiated and 15 control, randomly assigned) 7 week old C57BL/6J “cage mate” mice were purchased from Charles River Laboratories (Frederick, MD) and kept at the Columbia University Irving Medical Center animal facility for one week of adaptation. Glass-encapsulated TLD rods were injected at 8 weeks of age as described in<sup>26</sup>.

Animals were then placed in the VADER, provided with food and water ad libitum and kept on a 12:12 h light–dark schedule. For exposures longer than 1 week, the mouse “hotel” was removed from the VADER and mice transferred to a clean “hotel” with fresh bedding, food and water every 5–7 days. During this transfer, mice were outside the irradiator for a total of 5 min. Control mice were placed in an identical “hotel” in the same room and were transferred to a clean “hotel” roughly an hour before the irradiated mice. Temperature and humidity were monitored in both “hotels”.

Most experiments performed over the 1st year of operation of the VADER consisted of multiple runs where 15 mice were placed in the VADER and 3–5 mice removed at each time point. For long (1 month) irradiations, the early time points (<1 week) were performed in one run and the later time points in an independent run allowing more mice per time point. More recently, we have used a previously described portable incubator<sup>27</sup> to perform 2–3 day irradiations of blood at dose rates of 1 Gy/day. We have also begun more systematic studies using mice, irradiated at fixed dose rates of 1 Gy/day.

**Cell counts.** Peripheral whole blood samples were collected at euthanasia from each mouse by cardiac puncture using a heparin-coated syringe. The spleen was excised and homogenized and the isolated splenocytes were suspended in PBS 2% FBS. 20 µl of heparinized blood or spleen suspension was diluted to 200 µl in RBC lysis solution, stained with mouse CD45 antibody (WBC marker, clone 30-F11, eBioscience, San Diego, CA) and analyzed using flow cytometry (CytoFLEX, Beckman Coulter, Pasadena, CA).

**Apoptosis.** Peripheral blood cells and splenocytes were fixed using the FIX & PERM Cell Permeabilization Kit (Thermo Fisher Scientific, Waltham, MA) and stained with nuclear dye DRAQ5 (Thermo Fisher Scientific, Waltham, MA). The cells were measured using the ImageStreamX Mark II Imaging Flow Cytometer (Luminex Corporation, Austin, Texas). Images of 5000 cells per sample were acquired at 40X magnification using the 488 nm excitation laser. Captured images were analyzed using IDEAS (Luminex Corporation, Austin, Texas) software for measuring proportion of apoptotic cells, as identified by automated image analysis based on nuclear imagery features in combination with bright field morphology<sup>28</sup>. Data was expressed as mean and standard deviation and were analyzed using GraphPad Prism 6.0 (GraphPad Software, San Diego, CA, USA). The Kruskal–Wallis test was performed to compare data among all study groups. The Mann–Whitney *U* test was used to compare between two groups.  $P < 0.05$  was considered statistically significant.

**One week study.** The first VADER experiment focused on system validation. eleven mice were housed in the VADER mouse “hotel” (with four controls in a second “hotel”, in the same room). The VADER was programmed to produce the dose profile show in Fig. 7 and Table 1, mimicking the dose and dose rate kinetics after

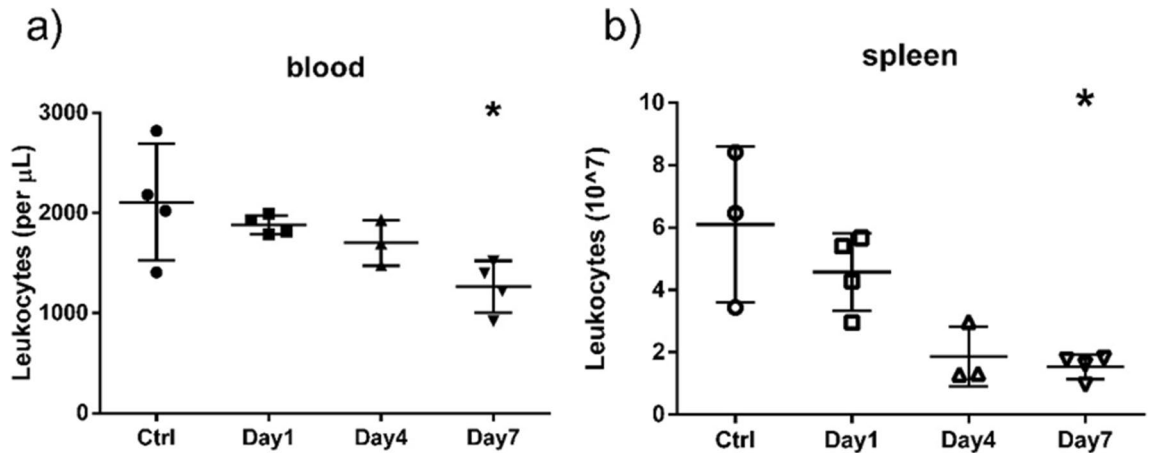


**Figure 8.** Leukocyte (CD45+) counts in (a) peripheral blood and (b) spleen, following irradiation using the protocol shown in Fig. 7. Symbols correspond to individual mice; the center line and error bars are average and Standard deviation. Asterisk denotes  $p < 0.05$  compared to control.

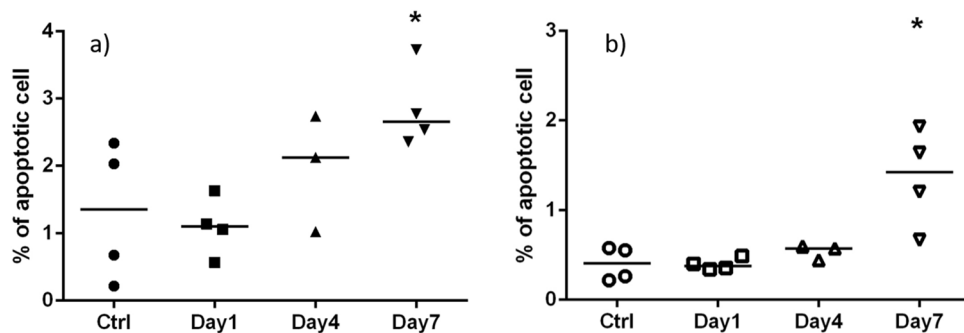


**Figure 9.** Fraction of apoptotic cells in (a) peripheral blood and (b) spleen, following irradiation using the protocol shown in Fig. 7. Symbols correspond to individual mice; the center line and error bars are average and Standard deviation. Asterisk denotes  $p < 0.05$  compared to control.

injection of 6.66 MBq  $^{137}\text{CsCl}_{(\text{aq})}^{15}$ . Four irradiated and two control mice were sacrificed at 24 h, three irradiated and one control on day 4 and the remaining four irradiated and one control mouse were sacrificed on day 7. Blood leukocyte and splenocyte cell counts (CD45+ cells) are shown in Fig. 8. As expected, the cell counts decreased with increasing absorbed dose over the irradiation period. Due to the large variation in the control mice, only the day 7 leukocyte and splenocyte counts were significantly lower than the control ( $p < 0.05$ ).

The apoptosis frequency in the mouse peripheral blood leukocytes and splenocytes, respectively is shown in Fig. 9. Although the overall rate of formation of apoptotic cells was relatively low ( $< 3\%$ ), there was a significant ( $p < 0.05$ ) increase in apoptotic blood leukocytes by day 7 (dose = 4.33 Gy) and in splenocytes by day 4 (dose = 2.5 Gy) and a further increase by day 7.

**One month study.** Figure 10 shows the measured dose, dose rate, temperature and humidity during one of the 30 day studies. As the VADER mouse “hotel” is limited to a capacity of 15 mice, experiments were run separately for the early and late time points. Figure 10 shows a run where time points of 5, 20 and 30 days were assessed.

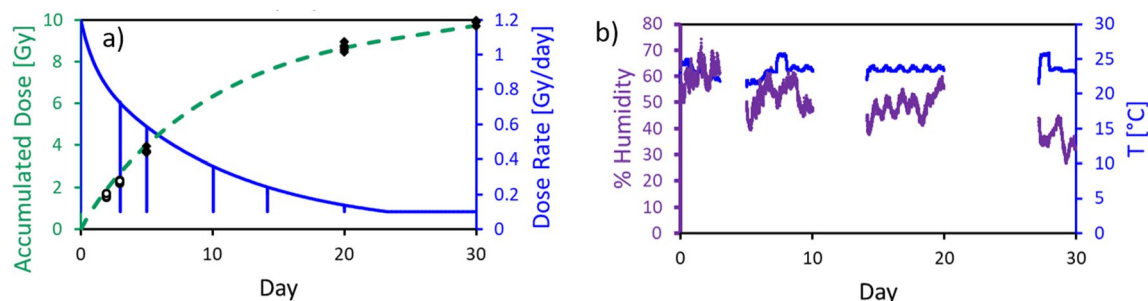
The measured dose rate, reconstructed from source position, was confirmed by the per-mouse TLD dosimetry and matched the required dose points. Temperature and humidity were within the accepted parameters. The decline in humidity is likely due to removal of 1/3 of the mice on days 5 and 20 (air flow into the mouse “hotel” was not humidified).

Figure 11 and Table 2 show the leukocyte counts for this study, which declined similarly to those in Fig. 8a with the beginning of recovery evident at Day 20–30.

## Discussion

We present here a novel low-dose-rate irradiator based on re-purposed  $^{137}\text{Cs}$  brachytherapy seeds. The irradiator was designed to mimic internal or external exposures from high level environmental  $^{137}\text{Cs}$  contamination, resulting in chronic exposures of Gy-level doses over days to weeks of exposure. Thus, the VADER was designed to provide dose rates of 0.1–1 Gy/day. Obtaining a wider range of doses can be achieved by building a taller structure, allowing the sources to be retracted further from the mice, but due to the  $1/r^2$  decrease of dose rate the





**Figure 10.** (a) Dose rate (solid line, right axis) and cumulative dose (dashed line, left axis) calculated from source position over a 30-day study. The vertical lines in the dose rate curve correspond to brief VADER openings for “hotel” cleaning and removing mice for analysis. Symbols at days 2, 3, 5, 20 and 30 are individual TLD readings for 5 mice at each time point (open symbols from a separate 5-day study using the same dose profile, conducted immediately prior to the 30-day study). (b) Measured humidity (thick purple line, left axis) and temperature (thin blue line, right axis) in one of the “hotels” used for the VADER. The gaps represent times when a different “hotel” was in use.

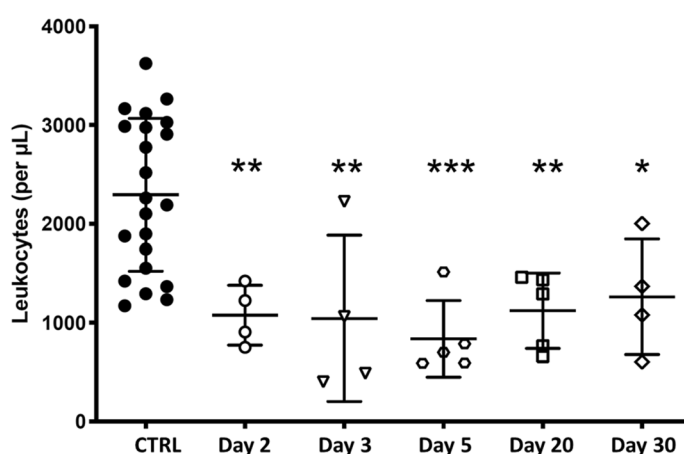


**Figure 11.** Leukocyte (CD45+) counts at various times during a 30-day study. Symbols correspond to individual mice; the center line and error bars are average and standard deviation. Single, double and triple asterisks denote  $p < 0.05$ ,  $p < 0.001$  and  $p < 0.001$ , compared to control, respectively.

Day	Dose rate [Gy/day]	Nominal dose [Gy]	Average TLD dose [Gy]	Leukocyte counts	p value
Control	0	0	$-0.05 \pm 0.08$	$2300 \pm 800$	NA
2	0.82	1.9	$1.6 \pm 0.1$	$1100 \pm 300$	0.005
3	0.72	2.7	$2.3 \pm 0.1$	$1000 \pm 800$	0.007
5	0.59	4.0	$3.7 \pm 0.1$	$800 \pm 400$	0.0004
20	0.14	8.7	$8.7 \pm 0.2$	$1100 \pm 400$	0.003
30	0.10	9.8	$9.95 \pm 0.2$	$1300 \pm 600$	0.002

**Table 2.** Dose rates and doses for the 30-day study. The TLD average and standard deviation dose based on 5 mice each. P values are based on an unpaired t test, comparing to controls.

system would have to be too tall to fit in a standard room to gain significantly in this respect. Another option, for achieving lower dose rates, if required, is to remove some of the seeds or replace them with weaker ones, essentially scaling down all doses.

**Alternate technologies.** The validity of modeling internal  $^{137}\text{Cs}$  exposures with external exposures was demonstrated by others, using a cabinet type  $^{137}\text{Cs}$  irradiator equipped with a computer controlled mercury attenuator<sup>29,30</sup>. In that system a mercury reservoir is placed between a large (18 Ci)  $^{137}\text{Cs}$  source and a stack of mouse cages. The level of mercury in the reservoir is modified, varying the attenuation of  $\gamma$ -rays, achieving dose

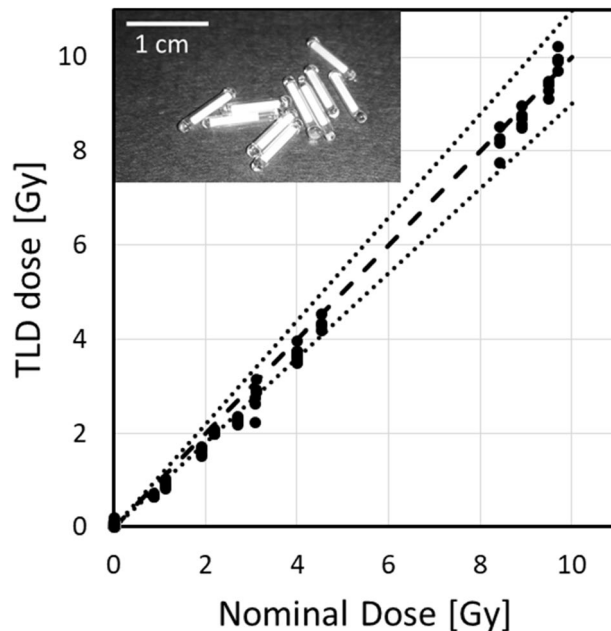


**Figure 12.** TLD reconstructed doses (in Gy) for mice irradiated in the VADER. Each point corresponds to an individual mouse dose. The dashed line is the identity and the dotted lines are  $\pm 10\%$ . The insert shows a photo of the encapsulated TLDs, reproduced from<sup>26</sup>, © Institute of Physics and Engineering in Medicine. Photo reproduced by permission of IOP Publishing. All rights reserved.

rates between approximately  $10^{-4}$  and  $0.25$  Gy/h<sup>29</sup>. This setup has been routinely used for calibration studies for internal emitter biomarker studies<sup>31–33</sup>.

An alternate approach to attenuation, which is likely to alter the energy spectrum of the source, is to place the source very far from the animals to be irradiated. An example of this approach is the NMBU FIGARO low dose rate facility in Norway<sup>34</sup>. FIGARO utilizes a  $^{60}\text{Co}$  source, providing a dose rate between  $3$  Gy/h, just outside the collimator and  $0.4$  mGy/h,  $20$  m away. The obvious drawback of such a system is that it requires a very large facility, which is not suited to an urban university/medical center. FIGARO to date has not published experiments using variable dose rates, though they could be easily achieved by periodically moving the animal cages. As dose rate varies with the distance from the source, care needs to be taken that the animals cannot move too much in this direction. This is not a huge problem when irradiating at a source distance of  $20$  m but becomes problematic for higher dose rates that require source distances of  $1$ – $2$  m.

**VADER performance.** *General.* At the time of writing this paper the VADER has been in operation for two years including three 30-day studies and thirteen shorter (3–7 day) runs, for the study of cytogenetic, proteomic, transcriptomic, and metabolomic endpoints. In addition to the design and dosimetry validation of the VADER we presented here blood count and apoptosis data from one 7-day study and one 30-day study. Additional manuscripts focusing on these different endpoints will be presented elsewhere (e.g.<sup>35</sup>). It should be noted that in our prior injection-based studies we were not able to access hematological data (especially at earlier time points) as the blood was too radioactive to analyze. Use of the VADER obviates this problem.

In the first pilot study (conducted in August 2018) the temperature in the VADER ranged from  $26$  to  $30$  °C. Temperature in the control “hotel” was slightly lower ( $23$ – $29$  °C), although both were somewhat warmer than the recommended temperatures for housing mice. Humidity in both “hotels” ranged from  $40$  to  $60\%$ . Following this week-long experiment, a second air conditioning unit was installed in the room, lowering summer temperatures to more acceptable levels. No temperature deviations were seen in any of the subsequent experiments.

During this pilot study we also discovered several errors in data logging, which were corrected. One power outage had been experienced, but the VADER control software had recovered successfully and resumed operation when the power was restored.

*Dosimetry.* An important aspect of performing these long-term studies, where mice are free to roam in a (possibly) spatially varying radiation field is individualized dosimetry. We have developed an *in vivo* dosimetry technique<sup>26</sup>, based on glass encapsulated TLD rods. The glass encapsulation allows the TLDs to be injected into mice without being damaged by the surrounding biofluids, while also allowing readout and annealing in the encapsulated state.

Figure 12 demonstrates *in vivo* measured doses, reconstructed using the TLDs, as a function of the nominal (requested) dose. The data show good agreement at the higher doses but the TLD doses were slightly lower than nominal at the lower doses. This may be due to the fact that most low doses were delivered in a short time using

the highest dose rate setting, where there is considerable spatial variation of dose at dose rates above 1 Gy/day, and it is possible that mice spent more time in the lower dose areas.

**Preliminary data.** The data above represent the first two runs of the VADER. Both runs utilized a dose/time profile measured in our prior  $^{137}\text{Cs}$  injection studies<sup>15–18</sup> tracking mice over 1 week or 1 month. Leukocyte depletion kinetics showed a nadir around day 3–7, similar to that seen for acute exposures<sup>36</sup>. The results show that leukocyte levels have not fully recovered by day 30, as is seen in acute exposures<sup>36</sup>. This is likely because the animals are continuously irradiated after the nadir. The low dose rate (below 0.3 Gy/day after day 7), results in a low rate of cell killing combined with the repopulation, thus delaying the full recovery of leukocyte numbers.

The main goal of the 30 day experiment was to mimic the injected  $^{137}\text{Cs}$  experiments reported previously<sup>16</sup>, indeed, both the pattern of up and down regulated genes and the metabolic profiles seen in that study was reproduced in this experiment and two subsequent repeats (manuscripts in preparation).

## Conclusions

We describe a low dose irradiation facility based on repurposed  $^{137}\text{Cs}$  brachytherapy seeds. The VADER provides dose rates between 0.1 and 1.2 Gy/day to up to 15 mice at a time. Environmental conditions suitable for housing mice are maintained in the VADER for weeks at a time allowing protracted experiments with short weekly breaks for “hotel” cleaning and replenishment of food and water.

The system is currently in routine use at Columbia University and can reproduce the results of  $^{137}\text{Cs}$  injection experiments without the complications and costs involved in the handling of radioactive reagents, animals, and biofluids.

Received: 20 March 2020; Accepted: 3 November 2020

Published online: 16 November 2020

## References

- Simon, S. L., Bouville, A. & Beck, H. L. The geographic distribution of radionuclide deposition across the continental US from atmospheric nuclear testing. *J. Environ. Radioact.* **74**, 91–105 (2004).
- Homeland Security Council, National planning scenarios (final version 21.3) (Washington DC 2006).
- Yasunari, T. J. *et al.* Cesium-137 deposition and contamination of Japanese soils due to the Fukushima nuclear accident. *Proc. Natl. Acad. Sci. USA* **108**, 19530–19534 (2011).
- Buddemeier, B.R. & Dillon, M.B., Key response planning factors for the aftermath of nuclear terrorism. (Lawrence Livermore National Laboratory, Livermore, 2009).
- Komura, K. *et al.* Pu isotopes,  $^{241}\text{Am}$  and  $^{137}\text{Cs}$  in soils from the atomic bombed areas in Nagasaki and Hiroshima. *J. Radiat. Res.* **26**, 211–223 (1985).
- Brandao-Mello, C. E., Oliveira, A. R., Valverde, N. J., Farina, R. & Cordeiro, J. M. Clinical and hematological aspects of  $^{137}\text{Cs}$ : The Goiania radiation accident. *Health Phys.* **60**, 31–39 (1991).
- Merz, S., Shozugawa, K. & Steinhauser, G. Analysis of Japanese radionuclide monitoring data of food before and after the Fukushima nuclear accident. *Environ. Sci. Technol.* **49**, 2875–2885 (2015).
- Hoshi, M. *et al.* Fallout radioactivity in soil and food samples in the Ukraine: Measurements of iodine, plutonium, cesium, and strontium isotopes. *Health Phys.* **67**, 187–191 (1994).
- Poeton, R. W., Glines, W. M. & McBaugh, D. Planning for the worst in Washington State: Initial response planning for improvised nuclear device explosions. *Health Phys.* **96**, 19–26 (2009).
- Buddemeier, B. R. Nuclear detonation fallout: Key considerations for internal exposure and population monitoring. (Lawrence Livermore National Lab. (LLNL), Livermore, (United States), 2018).
- Glasstone, S. & Dolan, P. J. The effects of nuclear weapons. Third edition. (Department of Defense, Washington, D.C. (USA); Department of Energy, Washington, D.C. (USA), 1977).
- Leggett, R. W. Biokinetic models for radiocaesium and its progeny. *J. Radiol. Prot.* **33**, 123–140 (2013).
- Thompson, D. F. & Church, C. O. Prussian blue for treatment of radiocesium poisoning. *Pharmacotherapy* **21**, 1364–1367 (2001).
- Turner, H. C. *et al.* Gamma-H2AX kinetic profile in mouse lymphocytes exposed to the internal emitters cesium-137 and strontium-90. *PLoS ONE* **10**, e0143815 (2015).
- Turner, H. C. *et al.* Effect of dose and dose rate on temporal  $\gamma$ -H2AX kinetics in mouse blood and spleen mononuclear cells in vivo following Cesium-137 administration. *BMC Mol. Cell Biol.* **20**, 13 (2019).
- Paul, S. *et al.* Gene Expression response of mice after a single dose of  $^{137}\text{Cs}$  as an internal emitter. *Radiat. Res.* **182**, 380–389 (2014).
- Goudarzi, M. *et al.* Development of urinary biomarkers for internal exposure by cesium-137 using a metabolomics approach in mice. *Radiat. Res.* **181**, 54–64 (2014).
- Goudarzi, M. *et al.* Metabolomic and lipidomic analysis of serum from mice exposed to an internal emitter, cesium-137, using a shotgun LC–MS(E) approach. *J. Proteome Res.* **14**, 374–384 (2015).
- Tapner, D. N., Nold, M. M. & Comar, C. L.  $\text{Cs}^{137}$  dose measurements in tissue—I. *Health Physics* **8**, 207–216 (1962).
- Thoraeus, R. Attenuation of gamma radiation from  $^{60}\text{Co}$ ,  $^{137}\text{Cs}$ ,  $^{192}\text{Ir}$ , and  $^{226}\text{Ra}$  in various materials used in radiotherapy. *Acta Radiol. Ther. Phys. Biol.* **3**, 81–86 (1965).
- Garty, G. *et al.* Mice and the A-Bomb: Irradiation systems for realistic exposure scenarios. *Radiat. Res.* **187**, 475–485 (2017).
- Bateman, T. J., Davy, T. J. & Skeggs, D. B. Five years hospital experience with the Amersham caesium 137 manual afterloading system. *Br. J. Radiol.* **56**, 401–407 (1983).
- Bertucci, A., Smilenov, L. B., Turner, H. C., Amundson, S. A. & Brenner, D. J. In vitro RABIT measurement of dose rate effects on radiation induction of micronuclei in human peripheral blood lymphocytes. *Radiat. Environ. Biophys.* **2**, 1–7 (2016).
- National Council on Radiation Protection & Measurements, Structural shielding design and evaluation for megavoltage x- and gamma-ray radiotherapy facilities. (Bethesda, MD, 2005).
- Mendez, I., Peterlin, P., Hudej, R., Strojnik, A. & Casar, B. On multichannel film dosimetry with channel-independent perturbations. *Med. Phys.* **41**, 011705 (2014).
- Garty, G., Pujol-Canadell, M. & Brenner, D. J. An injectable dosimeter for small animal irradiations. *Phys. Med. Biol.* **64**, 18NT01 (2019).
- Ghandhi, S. A., Smilenov, L. B., Elliston, C. D., Chowdhury, M. & Amundson, S. A. Radiation dose-rate effects on gene expression for human biodosimetry. *BMC Med. Genom.* **8**, 22 (2015).

28. Wang, Q. *et al.* Automated triage radiation biodosimetry: Integrating imaging flow cytometry with high-throughput robotics to perform the cytokinesis-block micronucleus assay. *Radiat. Res.* **191**, 342–351 (2019).
29. Howell, R. W., Goddu, S. M. & Rao, D. V. Design and performance characteristics of an experimental cesium-137 irradiator to simulate internal radionuclide dose rate patterns. *J. Nucl. Med.* **38**, 727–731 (1997).
30. Pasternack, J. B. & Howell, R. W. RadNuc: A graphical user interface to deliver dose rate patterns encountered in nuclear medicine with a <sup>137</sup>Cs irradiator. *Nucl. Med. Biol.* **40**, 304–311 (2013).
31. de Toledo, S. M. *et al.* Adaptive responses to low-dose/low-dose-rate gamma rays in normal human fibroblasts: The role of growth architecture and oxidative metabolism. *Radiat. Res.* **166**, 849–857 (2006).
32. Bishayee, A. *et al.* Marrow-sparing effects of 117mSn(4+)diethylenetriaminepentaacetic acid for radionuclide therapy of bone cancer. *J. Nucl. Med.* **41**, 2043–2050 (2000).
33. Lenarczyk, M., Goddu, S. M., Rao, D. V. & Howell, R. W. Biologic dosimetry of bone marrow: Induction of micronuclei in reticulocytes after exposure to <sup>32</sup>P and <sup>90</sup>Y. *J. Nucl. Med.* **42**, 162–169 (2001).
34. Lind, O. C., Oughton, D. H. & Salbu, B. The NMBU FIGARO low dose irradiation facility. *Int. J. Radiat. Biol.* **95**, 76–81 (2018).
35. Wang, Q. *et al.* DNA damage response in peripheral mouse blood leukocytes in vivo after variable, low-dose rate exposure. *Radiat. Environ. Biophys.* **59**, 89–98 (2020).
36. Ghosh, S. P. *et al.* Amelioration of radiation-induced hematopoietic and gastrointestinal damage by Ex-RAD<sup>®</sup> in mice. *J. Radiat. Res.* **53**, 526–536 (2012).

### Author contributions

G.G., Y.X., G.W.J., L.B.S. and D.J.B. designed the VADER. G.W.J., R.M. and D.C. manufactured and assembled the VADER. G.G., S.K.J. and R.S. loaded the Cs sources into the VADER. T.L.M. and P.J.C. consulted on safety and performed radiation surveys. S.A.A., A.J.F. and L.B.S. designed the animal studies, L.B.S., M.P.C. and C.B. handled the mice, H.C.T., S.A.G., S.R.M. and E.C.L. analyzed the samples, Q.W., M.P.C., H.C.T. and G.G. analyzed the data. G.G., T.L.M. and D.J.B. wrote the manuscript, Q.W. and M.P.C. prepared Figs. 8, 9 and 11. GG prepared the rest of the figures. All authors with the exception of Y.X. read and approved the manuscript.

### Funding

This work was supported by the National Institute of Allergy and Infectious Diseases (NIAID), National Institutes of Health (NIH) [Grant number U19 AI067773 to the Center for High-Throughput Minimally Invasive Radiation Biodosimetry]. The content is solely the responsibility of the authors and does not necessarily represent the official views of NIAID or NIH. Neither NIH nor NIAID were involved in study design, collection, analysis or interpretation of data. They were not involved in writing this manuscript or the decision to submit the article for publication.

### Competing interests

The authors declare no competing interests.

### Additional information

**Correspondence** and requests for materials should be addressed to G.G.

**Reprints and permissions information** is available at [www.nature.com/reprints](http://www.nature.com/reprints).

**Publisher's note** Springer Nature remains neutral with regard to jurisdictional claims in published maps and institutional affiliations.



**Open Access** This article is licensed under a Creative Commons Attribution 4.0 International License, which permits use, sharing, adaptation, distribution and reproduction in any medium or format, as long as you give appropriate credit to the original author(s) and the source, provide a link to the Creative Commons licence, and indicate if changes were made. The images or other third party material in this article are included in the article's Creative Commons licence, unless indicated otherwise in a credit line to the material. If material is not included in the article's Creative Commons licence and your intended use is not permitted by statutory regulation or exceeds the permitted use, you will need to obtain permission directly from the copyright holder. To view a copy of this licence, visit <http://creativecommons.org/licenses/by/4.0/>.

© The Author(s) 2020